Future Journal of Pharmaceutical Sciences

RESEARCH

Open Access

Enhanced therapeutic approach for diabetic foot ulcers: comparative study and characterisation of mupirocin-loaded nanosponge gel with marketed formulation for accelerating wound healing and in vivo evaluation

Rushikesh S. Dhamak[1*], Pramod S. Salve[1], Deepak R. Tiwari[1], Pradnya A. Raut[1] and Darshan S. Waghmare[1]

Abstract

Background The current investigation aimed to develop, optimise, and assess a mupirocin-loaded nanosponge-based topical delivery system for diabetic foot ulcer and to achieve prolonged drug release while improving drug deposition within the skin. The nanosponges carrying mupirocin were formulated using the emulsion solvent diffusion method. A 3^2 factorial design was utilised to investigate effect of two factors, specifically the concentration of ethyl cellulose and the stirring rate, on the physical attributes of the nanosponges. The optimised nanosponge formulation batch (F9) was subsequently incorporated into a Carbopol gel base, ensuring the desired physical attributes were achieved in the gel formulation containing nanosponges. The research included in vitro drug release evaluation, ex vivo drug deposition analysis, assessment of the antimicrobial action of the nanosponge formulation, and in vivo diabetic wound healing.

Results Drug polymer compatibility analysis was conducted using FT-IR spectroscopy revealed no interactions among mupirocin and ethyl cellulose molecules. Further FT-IR spectroscopy, DSC spectroscopy, and XRD spectroscopy analysis of optimised formulation batch revealed that the drug was successfully entrapped in nanosponges. Scanning electron microscopy confirmed the spherical and porous nature of the prepared nanosponges. The drug release pattern across the cellulose dialysis membrane followed a diffusion-controlled release pattern, and the drug deposition analysis exhibited substantial retention of mupirocin in the skin from the nanosponges formulation for up to 24 h. Furthermore, the optimised nanosponges gel formulation demonstrated stability and non-irritant properties, as indicated by the HET-CAM test. In vivo evaluation of wound healing activity in a Streptozotocin-induced diabetes mellitus with excision wound model revealed significant actions pertaining to wound healing and closure after 16 days of treatment.

Conclusion The mupirocin-loaded nanosponge gel contributed to remarkable and swift recovery and closure of wounds in diabetic rats. The nanosponges, acting as carriers for mupirocin, facilitated the effective delivery

*Correspondence:
Rushikesh S. Dhamak
rushikeshdhamak@gmail.com
Full list of author information is available at the end of the article

of the drug to the wound area, while the gel fostered an optimally humid environment conducive to wound care during the final stages of wound healing and sealing.

Keywords Mupirocin, Nanosponge gel, Streptozotocin, Sustained release, Topical delivery, Diabetic wound healing, Diabetic foot ulcer, Excision wound model

Graphical abstract

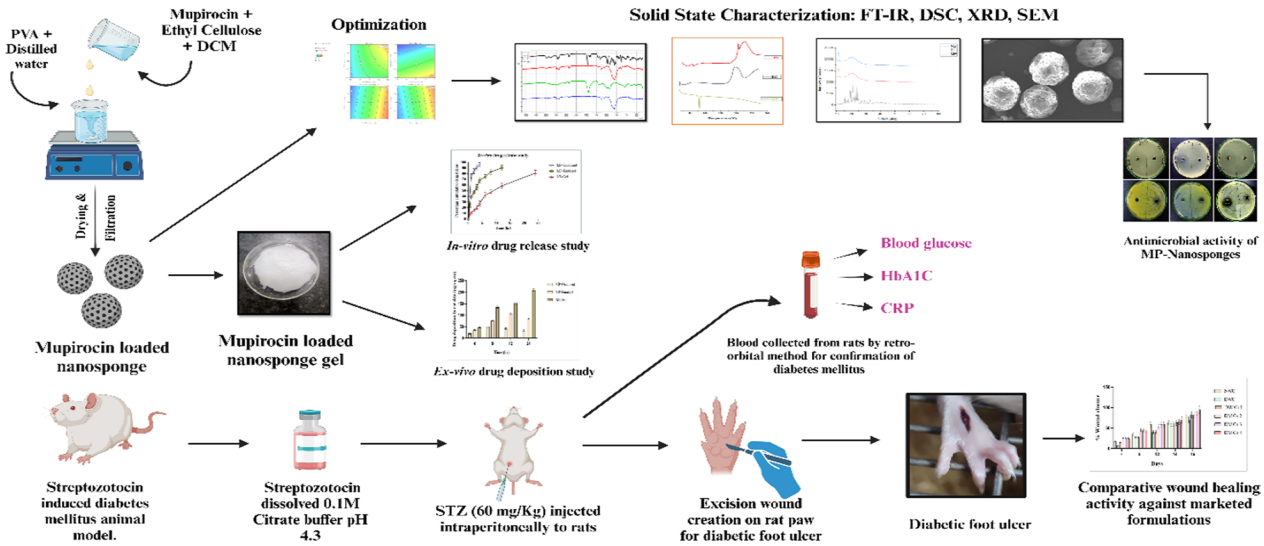

Background

Diabetes mellitus (DM) encompasses a cluster of persistent metabolic disorders marked by high blood glucose levels stemming from either inadequate insulin production or resistance to its effects [1]. The two clinically distinct types are type 1, caused by autoimmune beta-cell destruction resulting in complete insulin deficiency, and type 2, characterized by increased resistance to insulin action and insufficient insulin production [2]. Type 2 Diabetes Mellitus (T2DM) is the predominant form of diabetes, accounting for over 90% of cases globally. It is characterised by low insulin production and tissue insulin resistance [3]. The global prevalence of diabetes is rising, with projections estimating over 1.31 billion people will be affected by 2050 [4, 5].

Diabetic foot ulcers (DFUs) are substantial complications of diabetes, distinguished by ulceration linked with neuropathy and/or peripheral arterial disease [6–8]. DFUs can lead to severe complications such as infections, amputations, and mortality. Infections are observed in up to 58% of patients with new foot ulcers [9]. The prevalence of DFUs is higher in males (4.5%) than in females (3.5%) and in type 2 diabetics (6.4%) compared to type 1 diabetics (5.5%) [10]. Patients with diabetes experience varying foot sensitivity symptoms, ranging from pain and tingling in the early stages to numbness and toe weakening in the later stages [11]. DFUs are challenging to heal due to the presence of microbial biofilms, elaborate societies of microscopic organisms encased in a self-generated matrix of extracellular polymeric substances (EPS) [12, 13]. Diabetic mouse models hold clinical significance in relation to diabetic ulcers, while the excision wound mouse model is pertinent to both acute and chronic wound healing. Interestingly, the excision wound healing model in mice has potential applicability in diabetic wound healing as well, achieved by inducing diabetes prior to initiating the wound [14].

Nanosponge-Based Topical Drug Delivery: Conventional drug therapy for DFUs faces limitations due to neuropathy, hindering drug delivery to the injured site. Nanotherapeutics, particularly nanosponge-based topical delivery systems, offer advantages for chronic wounds like diabetic wounds, promoting effective wound healing and skin regeneration [15]. The proposed strategy involves preparing a mupirocin-loaded nanosponge topical dosage form capable of penetrating deeper tissue at the injured site. Mupirocin (Pseudomonic acid A), an antibiotic synthesised by Pseudomonas fluorescens, demonstrated pronounced efficacy against staphylococci and streptococci, as well as specific gram-negative bacteria

like Haemophilus influenzae and Neisseria gonorrhoeae. Additionally, it supports wound healing by promoting keratinocyte proliferation and augmenting growth factor production. The therapeutic benefits of mupirocin (MP) can be enhanced by synergistically integrating it with other substances and implementing innovative approaches [16–19]. Nanosponges (NSs) are nanosized sponge-like structures with numerous cavities capable of accommodating payloads [20]. NSs exhibit self-sterilising properties due to their average pore size of 0.25 µm, effectively preventing bacterial penetration. Additionally, they enhance drug bioavailability and improve the solubility of poorly soluble drugs [21]. They present several advantages over microsponges, including smaller particle size (below 500 nm), enhanced stability (up to 300 °C), and lipophilicity, which allows masking unpleasant flavours and transforming the physical state of drug from liquid to solid [22]. This unique drug delivery technology holds promise for attaining controlled and extended drug release, addressing the challenges of conventional topical delivery systems for diabetic wound healing.

Materials and methods

Materials

MP was purchased from Horster Biotek, Pvt. Ltd., situated in Indore, India. Ethyl cellulose (EC), Carbopol 934 (CP 934), Polyvinyl alcohol (PVA), and Dichloromethane (DCM) were obtained from Loba Chemie Pvt. Ltd. in India. Every other substance and chemical employed were of analytical calibre.

Method

Fabrication of nanosponge (NSs)

The preparation of MP-loaded Nanosponge (MP-NSs) was done by the emulsion solvent diffusion (ESD) method. MP and EC were used in the ratios of 1:4, 1:6, and 1:8. The amount of MP was kept constant at 100 mg in the development of NSs. In the emulsion solvent diffusion method, the NSs were fabricated by incorporating different proportions of EC. The internal organic phase, consisting of MP and EC, was blended with 20 mL of dichloromethane (Alternative to DCM are Ethanol, Ethyl Acetate or Acetone) using ultrasonic agitation in an ultrasonicated bath (70 kHz frequency) for a duration of 2 minutes (Crest, Ultrasonic Corporation, Cortland, New York), and in the external aqueous phase of 100 mL of distilled water, 1 g of polyvinyl alcohol (PVA) was dissolved by heating up to 60 °C. Then the internal organic phase was dropwise added to the external aqueous phase while stirring at 1000 rpm for 2 hours (hrs), and the fabricated NSs were gathered by filtration followed by oven drying at 40 °C for 24 hrs [23].

Factorial experimentation and optimization using design of experiments (DoE) software

Initial experiments were conducted to investigate the effect of MP/EC ratios and stirring rates on the physical properties of NSs. Throughout all formulations, the concentration of MP, internal phase volume, and PVA concentration remained consistent. To optimise the dependent variables like production yield (PY), entrapment efficiency (EE), and mean particle size (MPS) of nanosponges, nine formulations were created using a 3^2-factorial design, with the independent variables being polymer concentration (X1) and stirring rate (X2) [24].

Physicochemical characterisation

Fourier transform infrared (FT-IR) spectroscopy analysis

FT-IR spectroscopy data of MP, EC, and optimised MP-NSs were recorded on an FT-IR spectrophotometer (Jasco FT-IR 6700) using the potassium bromide (KBr) press technique as per previously reported methods. Approximately 1–4 mg of sample was combined with dry KBr in a 1:1 ratio and scanned at transmission mode over 4000–400 cm^{-1} [25].

Thermal analysis by differential scanning calorimetry (DSC)

The thermal assessment of MP, EC, and MP-NSs was conducted using a differential scanning calorimeter (Mettler Toledo DSC, USA). Precisely measured quantities of samples (5 mg) were placed in aluminium containers and hermetically sealed. Each sample was subjected to a gradual temperature increase of 10 °C per minute within the temperature interval of 25–300 °C, all in a nitrogen environment [26].

Solid state characterisation

The X-ray diffraction (XRD) study was conducted to evaluate the solid-state character of the formulation. Powder XRD studies of MP, EC, and optimised MP-NSs were conducted using a powder X-ray diffractometer (Brucker D2 Phaser 2nd Gen). Samples were placed in the sample stage, and data were obtained over 2θ range from 5 to 50° using a step size of 0.019° per sec [27].

Particle size and zeta potential characterisation

The analysis of particle size for MP-NSs was executed employing the "Malvern Zetasizer NanoZS (Malvern Instruments, UK)". The specimen being investigated was diluted with distilled water (1:200) and introduced into a disposable polystyrene cuvette. The measurement of particle size and polydispersity index (PDI) was conducted based on the principles of dynamic light scattering (DLS). The identical procedure was adhered to for gauging zeta

potential (ZP), albeit employing an electrode cuvette. Each sample was subjected to triplicate testing ($n = 3$) [28].

Entrapment efficiency (%EE)

The ultracentrifugation technique was used to assess the entrapment efficiency of MP-NSs. Samples were centrifuged at 10000 rpm for 30 min using an ultracentrifuge (Remi C-24, Mumbai, India). Unentrapped MP content in the supernatant was diluted with an appropriate medium before being measured using a UV-visible spectrophotometer at 222 nm [29]. Entrapment efficiency was calculated as per Eq. (1).

$$\%EE = \frac{\text{weight of total drug} - \text{weight of free drug} \times 100}{\text{weight of total drug}} \quad (1)$$

Scanning electron microscopy (SEM) analysis

The structure of NSs was investigated utilising a scanning electron microscope (GEOL 5400, USA) with an operational voltage of 20 kV. Prior to observation, dehydrated NSs underwent a 45-s coating with a gold–palladium alloy in an argon atmosphere. The SEM image was captured at a magnification of 3000 [30].

In vitro antimicrobial study of optimised MP-NSs formulation

Generation of bacteria inoculums

Inoculum was standardised, and 106 colony-forming units (CFU/mL) of the required density were achieved. Nutritious broth (5 mL) was mixed with a loopful of the *Staphylococcus aureus, Escherichia coli, and Pseudomonas aeruginosa*, and the mixture was then cultured for 24 h at 3 °C. To standardise the culture to 106 CFU/mL (equal to 0.5 McFarland standards), 0.2 mL of the microbes 24-h culture were poured into 20 mL of sterilised nutritious broth and cultured for 3–5 h. Cultures of test microbes on agar–agar and 8% nutritional broth were combined to create Nutritional Broth Medium (NBM), which was used to cultivate the bacterial strains. It was autoclaved at 15 lbs. pressure for 25–30 min. On petri plates, 15 mL of NBM were poured to prepare agar test plates in an aseptic condition, then subjected to stabilisation at room tempertature (RT). In peptone saline solution, bacterial cell cultures were routinely subcultured and incubated at 37 °C for 24 h.

Agar plates and test sample preparation

The bacterial strains were inoculated onto sterile agar plates by streaking the swab across the entire surface of the agar 2–3 times to ensure uniform distribution of the inoculum. The agar plate was rotated at a 60° angle during this process. Subsequently, the plates were allowed to air-dry in a sterile environment at RT. Wells with a diameter of 9 mm were then carefully created in the plates under aseptic conditions. The preparation of the test samples (MP-NSs) at a concentration of 10 mg/mL and the reference drug Ciprofloxacin at 100 µg/mL in dimethyl sulfoxide (DMSO) was carried out. Using a sterile micropipette, 50 µL of both the reference and test samples were dispensed into the wells. The plates were positioned in an incubator adjusted to a temperature of 37 °C for a duration of 24 h and the zone of inhibition (ZOI) for each bacterial strain was measured in triplicate using a calibrated digital Vernier caliper.

Agar well diffusion method

By using this method, the antibacterial action of MP-NSs formulation was tested against *Staphylococcus aureus, Escherichia coli, and Pseudomonas aeruginosa.* These three microorganisms are most abundant in DFUs [31]. Sterile Muller Hinton plates of agar were formed, and wells of 6 mm were punched into the plates using a sterilised cup borer. The plates were swabbed with a 24 h culture of test organisms using sterile cotton swabs. To the wells, 100 µL of MP-NSs solution were added, and plates were subjected to incubation in an upward position at 37 °C for 24 h., after which the plates were checked for ZOI. Control was 100 µL of (10% v/v) DMSO solution. The experiment was performed in triplicate, and the mean of the zone sizes recorded was calculated.

Preparation of MP-loaded nanosponge gel

To prolong the retention time on the skin surface, an optimised formulation of MP-NSs was selected for conversion into a topical gel system. Carbopol-934 (0.5%w/v) was allowed to swell in double-distilled water for 12 h. The dry powder of MP-NSs (equivalent to 100 mg of the drug), propyl paraben (0.5%w/v), and methyl paraben (0.2%w/v) were added to 10 mL of propylene glycol, and the propylene glycol suspension was gradually added to the swelled CP-934 gel while continuously stirring to achieve a uniform mixture. To obtain a translucent gel, a 1:1 molar ratio of triethanolamine base and CP-934 was added to the homogenous mixture. This step was taken to ensure a well-mixed and visually appealing gel product [32].

Assessment of gel containing MP-nanosponges

Upon visual inspection of the gel for its texture, colour, and uniformity, a comprehensive evaluation was conducted on the following parameters:

pH measurement

The pH of the formulated gel was gauged using a pH metre that had been calibrated with a pH 7 buffer prior to use. The electrode tip was immersed in the gel, and the reading was taken after 2 min. This pH measurement procedure was performed in triplicate, and the average value was computed.

Spreadability analysis

The spreadability of the gel was determined by placing a known weight of the sample between two glass slides, and a weight of 500 g was applied over the slides for approximately 5 min, after which no further spreading was anticipated. The initial and final diameters of the spread circles were measured in centimetres, serving as comparative metrics for spreadability.

Viscosity measurement

Viscosity, which signifies a resistance of fluid to flow, was assessed using a Brookfield viscometer equipped with spindle No. 7, operating at various rotations per minute (rpm) at room temperature (RT).

Drug content analysis

1 g of MP-NSs gel was precisely weighed, dissolved in methanol, sonicated for 15 min, and then adjusted to the mark in a 100 mL volumetric flask using methanol. From this solution, 1 mL was withdrawn, further diluted to 10 mL with methanol, and then a final dilution was carried out using distilled water to achieve a concentration within the Beer's law range. The absorbance was measured at 222 nm using a UV spectrophotometer against a blank gel treated in the same manner as a sample [33].

In vitro drug release assay

In vitro drug release investigations were conducted using Franz diffusion cells with a receptor chamber capacity of 20 mL and an effective diffusion area of 3.14 cm2. A cellulose dialysis membrane from Himedia, Mumbai, India, was soaked in the receptor medium (phosphate buffer, pH 5.8) for a period of 24 h prior to the commencement of the experiment. The donor side of the arrangement held a predetermined quantity of gel containing MP-NSs. During the experiment, the receptor solution was consistently agitated at 50 rpm and maintained at a steady temperature of 32 ± 0.5 °C through a circulating jacket. At specific intervals, 1 mL samples were withdrawn from the receiving compartment, and an equal volume of fresh buffer was introduced to ensure sink conditions. The extracted samples were subjected to analysis using a UV-Spectrophotometer to quantify the quantity of released MP. To facilitate comparison, the release profiles of a conventional cream (Mupirocin Cream USP, 2%, Glenmark) and a commercially available MP ointment (T-bact, GlaxoSmithKline) formulation were also examined. The drug release data underwent linear regression analysis to determine the release kinetics, encompassing zero-order and first-order release kinetics, as well as the diffusion-controlled mechanism (Higuchi model). [34].

Ex-vivo drug deposition assay

A study involving drug deposition within the skin was conducted using a Franz diffusion cell and excised rat abdominal skin. The outer layer of the skin was exposed to the surrounding environment, while the inner layer faced the solution in contact. The surface of the skin facing the outside environment was the epidermal side, whereas the dermal side was directed towards the solution in contact. The receptor compartment was filled with 20 mL of phosphate buffer at pH 5.8, maintained at a temperature of 33 ± 0.6 °C, and agitated at a rate of 50 rpm. Prior to the application of the sample, the skin was saturated with the diffusion medium for an hour. A 40-mg portion of the sample was applied to the donor compartment. For the quantification of the drug accumulated in the skin, the diffusion cell was disassembled after time intervals of 4, 8, 16, and 24 h. The skin was cautiously detached, and the mupirocin present on the surface was cleansed using distilled water [34].

Determining mupirocin concentrations in skin specimens

MP was recovered from the skin utilizing a technique outlined by Echevarria et al. [35]. In brief, the skin was fragmented into smaller sections and subsequently crushed and ground using 10 mL of methanol. Following this, the crushed mixture underwent a 15-min session of ultrasonication to ensure the comprehensive extraction of the drug. The methanolic extract that resulted was later centrifuged at a speed of 8,000 rpm for a duration of 15 min. The liquid portion above the sediment, which held the extracted substances, was meticulously gathered. This collected supernatant was then evaporated and subsequently mixed back with the suitable solvent. Prior to analysis, the sample was filtered using 0.2-µm Whatman filter paper and subjected to assessment using a UV spectrophotometer at 222 nm. Intact skin was enriched with predetermined quantities of the drug to determine the recovery rate of the drug from the skin Subsequently, the skin was fragmented into smaller sections, crushed, drug extracted, and analysed using the previously described procedure.

Skin irritation studies

The optimised gel formulation containing MP-NSs was subjected to skin irritation assessments using the HET-CAM (Hen's Egg Test-Chorioallantoic Membrane) technique [36]. Fertile white chicken eggs were sourced from commercial suppliers. Fresh eggs, which were nine days older and weighed between 50 and 60 g, were selected for the study. The irritation evaluation involved the negative control, which was sodium chloride (0.9%w/v NaCl), the positive control, which was sodium hydroxide (1%w/v NaOH), and the prepared MP-NSs gel. The HET-CAM test was used to assess irritation. The irritation scores from all treated groups were recorded at various time intervals, and the mean irritation score was calculated [37].

Stability studies

The MP-NSs gel was evaluated for its stability in an accelerated stability chamber (REMI) at three different temperatures (4 ± 2 ºC, 25 ± 2 ºC and 37 ± 2 °C) and 75% relative humidity (RH) for three months. The gel was evaluated for physical appearance, viscosity, pH, and Spreadability. Any change in appearance, pH, viscosity, or Spreadability of the stored MP-NSs gel was recorded [38].

In vivo wound healing activity

Wistar albino female rats in good health, weighing 180 and 250 g, were selected. The Institutional Animal Ethics Committee (Approval number IAEC/UDPS/2022/02/08) granted approval to the study protocol in accordance with Indian Committee for the Purpose of Control and Supervision of Experiments with Animals (CPCSEA) specifications. Throughout the study, animals were kept in a standard laboratory environment at a temperature of 25 ± 2 °C with a relative humidity of 44–56% and fed a standard diet and water.

Diabetes animal model

The described experimental protocol involved inducing diabetes mellitus in Wistar rats through the intraperitoneal (I.P.) delivery of streptozotocin (STZ) at a dose of 60 mg/kg body weight. Prior to the STZ injection, the rats were subjected to an overnight fasting period. To safeguard pancreatic beta cells from excessive harm induced by STZ, niacinamide was administered intraperitoneally at a dosage of 120 mg/kg body weight, 15 min prior to the STZ injection. [39, 40]. The STZ was prepared in a 0.1 M citrate buffer with a pH 4.5 for the I.P. injection. After 72 h from the STZ injection, blood samples were collected from the rats using the retro-orbital method, which involves obtaining blood from the blood vessels located behind the eye socket, a commonly used technique in small laboratory animals like rats. To confirm the successful induction of diabetes mellitus in the rats, various parameters were measured. These included HbA1C (glycated haemoglobin), blood glucose levels, and CRP (C-reactive protein) levels. These measurements were taken both before the induction of diabetes (baseline) and after 72 h following the STZ injection. The changes in these parameters would indicate the development of diabetes mellitus in the rats [41–43].

Excision wound model

Every rat participating in the study was administered an intraperitoneal injection of thiopentone sodium at a dosage of 40 mg/kg to induce anaesthesia on the day designated for wound creation. The wound development procedure involved creating a rectangular pattern on the upper side of the rat's paw. Using a scalpel blade, a wound was created by separating a complete skin layer with a standardised dimension of 2 mm × 5 mm. The rats were then randomly distributed into various experimental groups for further study. The purpose of this experimental setup was likely to be to investigate wound healing or other related phenomena in response to different treatments or interventions [44].

Animal groups and treatment protocol

Rats were split into 6 groups ($n = 5$), with 5 rats in each group, and exposed to the subsequent treatment:

Group I: Control group with normal wound (NWC), Non-Diabetic animal with wound received citrate buffer and distilled water.
Group II: Control group with Diabetic wound; Diabetic animals with wounds who received no treatment (DWC).
Group III: Diabetic wound treatment by MP-NSs gel formulation.
Group IV: Diabetic wound treatment by standard MP ointment (T-bact, GlaxoSmithKline).
Group V: Diabetic wound treatment by standard MP Cream (Mupirocin Cream USP, 2%, Glenmark).
Group VI: Diabetic wound treatment by standard Becaplermin gel (REGRANEX, Smith&Nephew).

Treatment was applied topically to treat excised wound area. This treatment was followed once a daily.

Determination of wound area, calculation of wound contraction

On predefined days 1, 4, 6, 8, 10, 12, and 16, a camera was used to document the progression of changes in the

wound location. Image analysis software computed the wound area from the pictures. By using Eq. (2), the percentage (%) of wound closure can be calculated [45].

$$\%\ \text{Wound closure} = \frac{[\text{Area of initial wound}) - \left(\text{N th day area of wound}\right) \times 100}{(\text{Area of initial wound})} \quad (2)$$

GraphPad Prism VIII was used to plot the graph showing the % of wound closure vs the number of days since the wound first developed.

Results

Formulation and optimization of nanosponges

The process of formulating nanosponges is presently restricted in terms of its intricacy and expense. Although certain nanosponges available on the market are manufactured through the suspension polymerization method, an alternative technique, referred to as the ESD method, has exhibited potential for nanosponge production. The ESD method is characterised by its simplicity, reproducibility, and efficiency, rendering it a fitting approach for generating MP-NSs. A noteworthy advantage of this method is its ability to bypass the use of toxic solvents. In order to assess the impact of various variables on % entrapment efficiency, % production yield, and mean particle size of nanosponges, a factorial design was employed alongside analysis of variance (ANOVA). The factors under consideration included the concentration of EC and the stirring rate, which were investigated to uncover their effects on the aforementioned parameters. Table 1 presents the coded levels of concentration of EC and stirring rate that were utilised in the experimental design. These coded levels served as the basis for investigating the impact of independent variables on dependent variables. Table 2 provides an overview of how the independent variables influenced these specific response variables, shedding light on the relationships and effects within the experimental framework. The visual representation of the data is facilitated through the utilisation of two- and three-dimensional surface plots. These plots elucidate the relationships between variables and response outcomes, these insightful visualisations are presented in Figs. 1 and 2. The regression equation (Eq. 3) for %EE is as follows:

$$Y1\ (\%EE) = 83.50 + 5.28A - 0.7783B \quad (3)$$

where, A represents the EC concentration and B represents the stirring rate. The results revealed that the concentration of EC had a notable positive influence on the drug entrapment efficiency (%EE), meaning that increasing the EC concentration led to higher drug entrapment. On the other hand, the stirring rate had a significant negative effect on %EE, indicating that higher stirring rates resulted in lower drug entrapment.

Table 1 Coded level of ethyl cellulose and stirring rate for experimental design

Coded level	Actual values	
	Ethyl cellulose (mg)	Stirring rate (rpm)
− 1	400	600
0	600	1000
+ 1	800	1400

Table 2 The effect of Mupirocin: Ethyl cellulose ratio and stirring rate on production yield, EE, and mean particle size

Batches	Factors		Responses		
	Mupirocin: Ethyl cellulose	Stirring rate	Particle size (nm)	Entrapment efficiency (%)	Production yield (%)
F1	100:400	600	335.4 ± 4.25	76.93 ± 1.02	63 ± 2.14
F2	100:600	600	381.5 ± 2.13	85.73 ± 0.98	61 ± 1.26
F3	100:800	600	451.8 ± 3.36	88.72 ± 2. 55	69 ± 3.49
F4	100:400	1000	263.4 ± 1.71	79.10 ± 1.43	73 ± 2.51
F5	100:600	1000	189.5 ± 2.21	84.48 ± 3.70	65 ± 1.87
F6	100:800	1000	304.1 ± 3.32	89.84 ± 1.93	77 ± 3.64
F7	100:400	1400	148.5 ± 2.19	77.7 ± 3.02	61 ± 3.91
F8	100:600	1400	202.2 ± 1.02	82.14 ± 1.47	76 ± 1.22
F9	100:800	1400	212.6 ± 3.05	86.87 ± 2.52	74 ± 2.37

[a] Each observation is the mean ± SD of three determinations

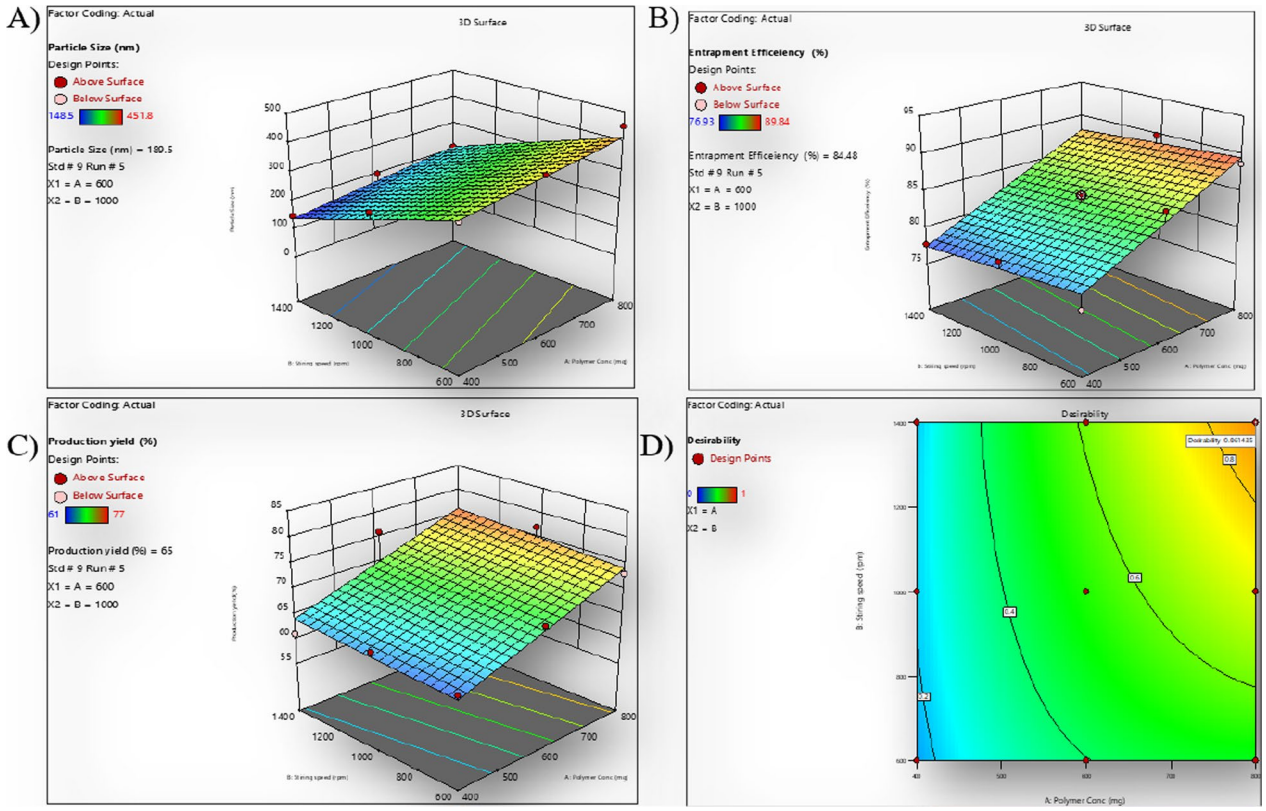

Fig. 1 Three-dimensional surface plots of **A** Entrapment efficiency, **B** Particle size, **C** Production yield and **D** Desirability plot

For particle yield (PY), a linear regression equation (Eq. 4) was generated, indicating that both the EC concentration and stirring rate had a positive influence:

$$Y2\ (PY)\ = 69.11 + 6.00A\ + 1.00B \tag{4}$$

Regarding mean particle size (MPS), a polynomial regression equation (Eq. 5) revealed that the EC concentration had a positive effect, while the stirring rate had a negative effect:

$$Y3\ (MPS)\ = 276.56 + 36.87A\ - 100.90B \tag{5}$$

Fit statistics for data analysis of response variables are given in Table 3. Based on the response surface methodology study, it was found that formulation (F9) performed better in terms of %EE, %PY, and MPS. Post-analysis confirmation at a two-tailed 95% confidence level is given in Table 4. As a result, the optimised nanosponges batch (F9) was selected for further characterisation studies and incorporated into a Carbopol gel base. The findings from the factorial design and regression equations provide valuable insights for optimising nanosponge formulations with enhanced properties for potential pharmaceutical applications.

Characterisation of nanosponges

FT-IR spectroscopy analysis was conducted on MP, EC, and the optimised MP-NSs formulation (F9). The resulting data, as depicted in Fig. 3, demonstrated that the key peaks of MP were similarly present in the physical combination of MP, EC, and CP. This outcome suggests the absence of substantial alterations or interactions among these components within the mixture. Consequently, this observation indicates the stability of the formulations.

Additionally, the FT-IR spectrum (as illustrated in Fig. 4) of the optimised nanosponge formulation (F9) exhibited all the significant peaks corresponding to EC, whereas the major peaks attributed to MP were conspicuously absent. This observation serves as confirmation that the MP has been effectively encapsulated within the nanosponges.

In order to investigate thermal characteristics, thermograms were acquired for MP, EC, and the optimised MP-NSs formulation, as depicted in Fig. 5. MP exhibited a distinct endothermic peak at 77.78 °C, signifying its melting point. Notably, EC and the optimised MP-NSs formulation displayed a broad exothermic peak at the same temperature, which indicated the absence of the original

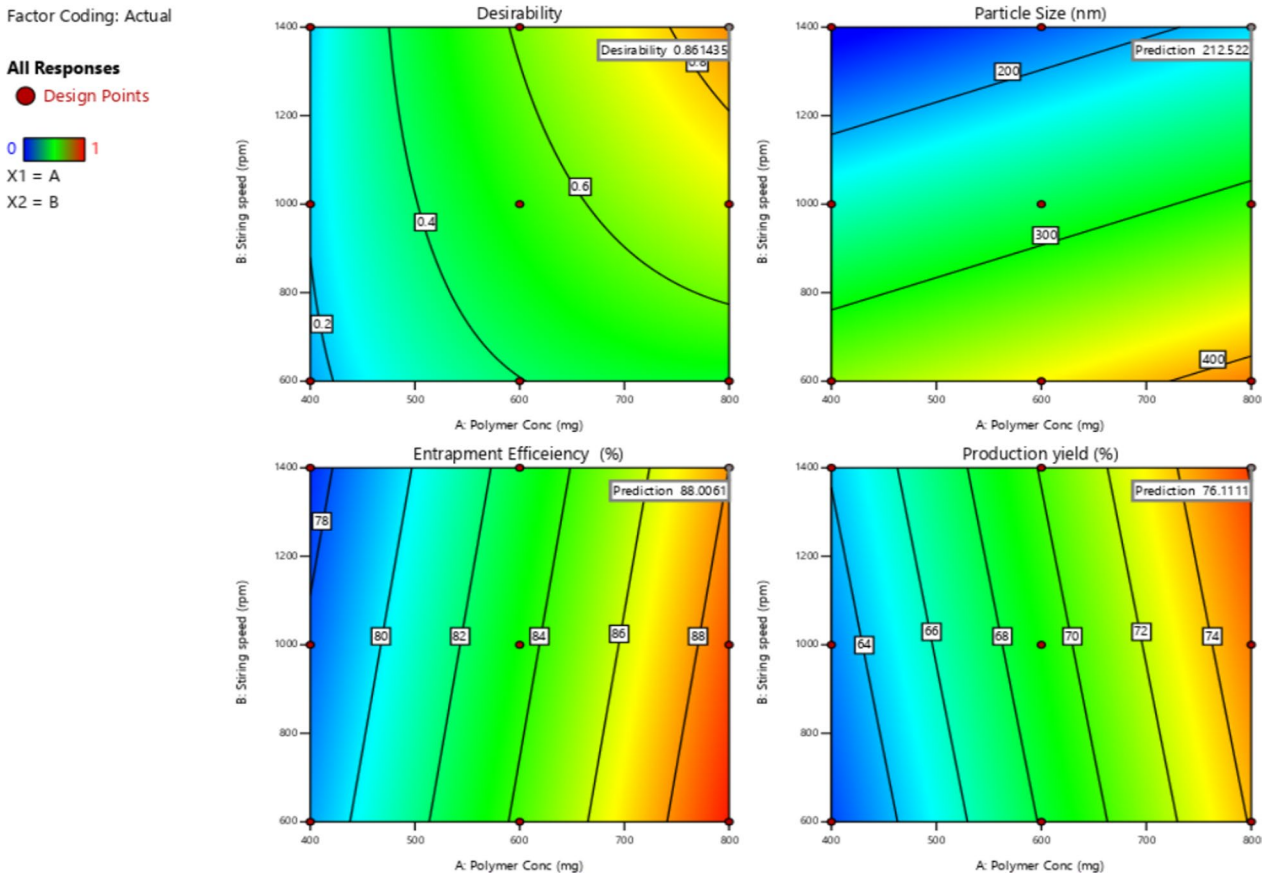

Fig. 2 Optimization of mupirocin entrapped nanosponge by desirability plot

Table 3 Fit statistics for data analysis of response variables using full factorial design

Fit statistics	Standard deviation	Mean	Coefficient of variation %	R^2	Adjusted R^2	Predicted R^2	Adeq precision
Particle size	41.78	276.56	15.11	0.8686	0.8248	0.7847	11.4220
Entrapment efficiency	1.39	83.50	1.67	0.9363	0.9151	0.8355	15.0809
Production yield	3.49	69.11	5.04	0.7528	0.6704	0.4910	6.9572

Table 4 Post Analysis confirmation at two tailed, 95% confidence level

Solution 1 of 5 response	Predicted mean	Predicted median	Observed	Standard deviation	SE mean	95% CI low for mean	95% CI high for mean	95% TI low for 99% Pop	95% TI high for 99% Pop
Particle size	212.52	212.522		41.7823	27.854	144.36	280.68	− 47.751	472.796
Entrapment efficiency	88.006	88.0061		1.39237	0.928	85.734	90.277	79.3326	96.6796
Production yield	76.111	76.1111		3.48542	2.3236	70.425	81.796	54.3995	97.8227

sharp peak. This observation strengthens the conclusion that MP has been efficiently encapsulated within the nanosponges.

The XRD graph (shown in Fig. 6) for MP displayed distinct sharp peaks, indicative of its crystalline structure. Conversely, both EC and the optimised MP-NSs

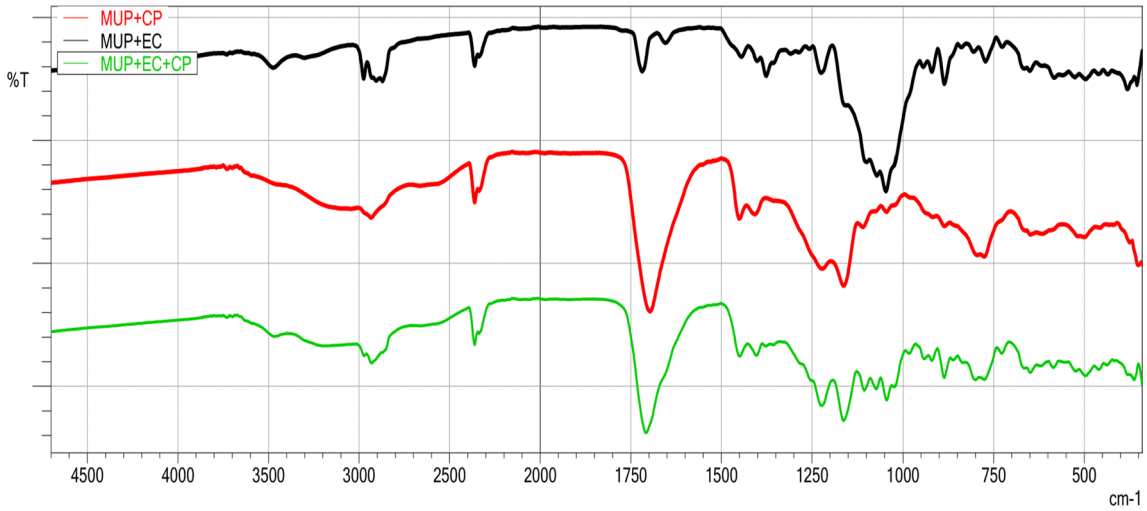

Fig. 3 FT-IR spectrum of physical mixture of mupirocin ethyl cellulose and carbopol 934

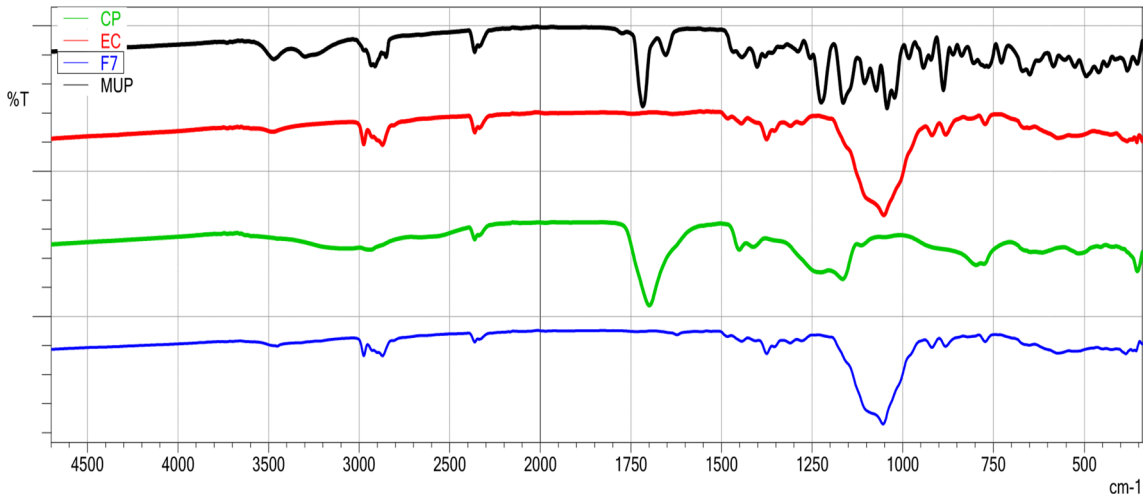

Fig. 4 FT-IR spectrum of ethyl cellulose, mupirocin, carbopol 934 and formulation batch (F9)

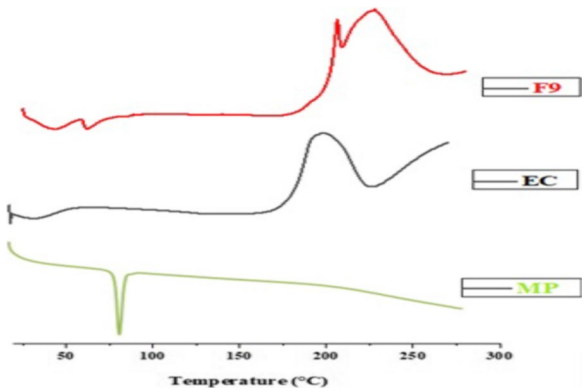

Fig. 5 DSC thermogram of mupirocin, ethyl cellulose and optimised formulation batch (F9)

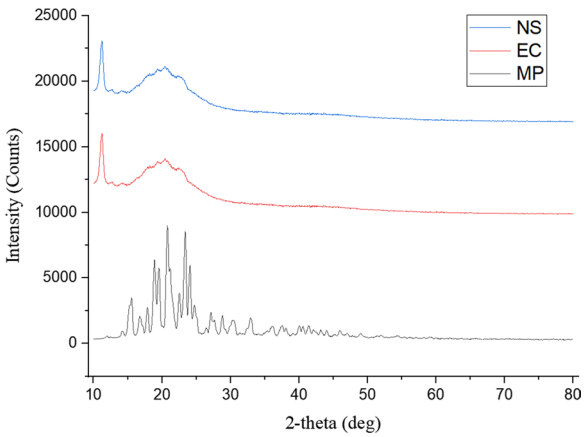

Fig. 6 X-ray diffraction (XRD) graph of mupirocin, ethyl cellulose and optimised formulation batch (F9)

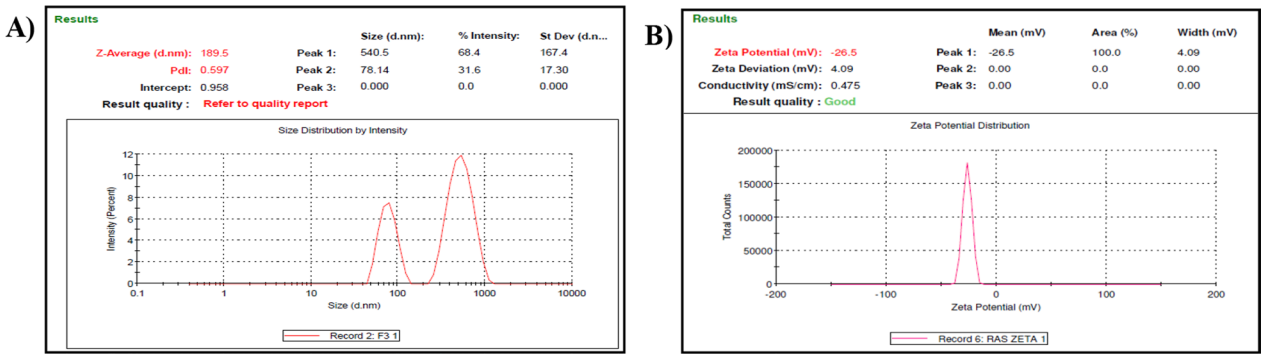

Fig. 7 Particle size **A** and zeta potential **B** of MP-NSs

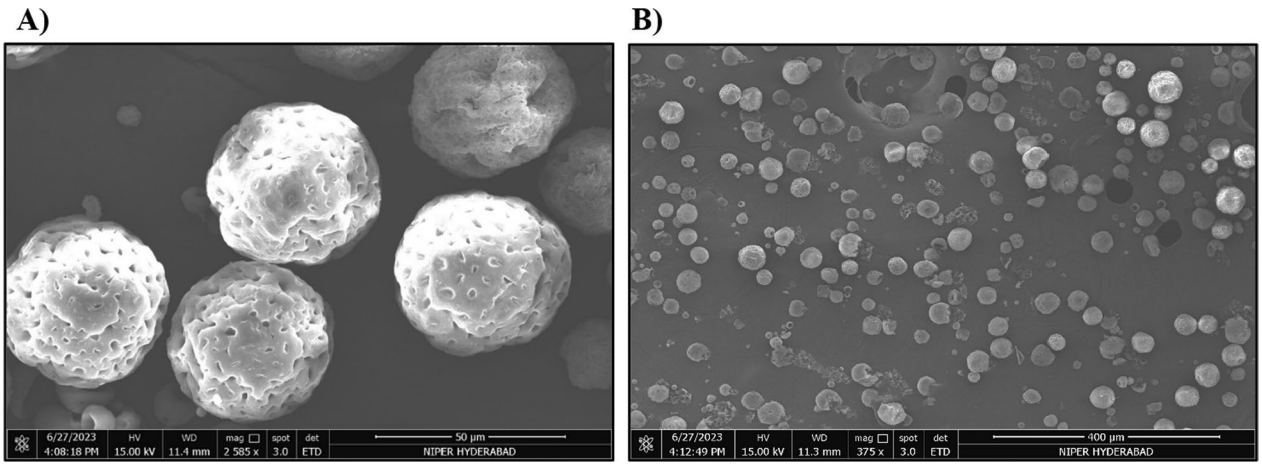

Fig. 8 Scanning Electron Microscopy images of **A** mupirocin-loaded nanosponges at × 2585 magnification **B** mupirocin-loaded nanosponges at × 375 magnification

exhibited an amorphous nature in the XRD pattern, providing additional verification of the successful encapsulation of the MP within the nanosponges. Moreover, the optimised MP-NSs were characterised by a mean particle size of 189 nm and a zeta potential value of (−) 26 mV, as depicted in Fig. 7.

SEM images of the MP-NSs, as shown in Fig. 8, revealed a consistent spherical morphology characterized by a porous structure. Notably, these images displayed no discernible intact Mupirocin crystals, providing strong visual evidence of the effective entrapment of the drug within the nanosponge matrix.

In an antimicrobial study, the antimicrobial efficacy of the MP-NSs formulation was assessed against commonly found bacterial strains (*Staphylococcus aureus, Escherichia coli, and Pseudomonas aeruginosa*) associated with diabetic foot ulcers. Employing the agar-well diffusion method, inhibitory potential of nanosponge formulation was determined. Figure 9 illustrates these results, which were then compared with those of the reference drug Ciprofloxacin and a control solution. Recorded zone of inhibition values against the targeted microorganisms are compiled in Table 5. To visually represent the antimicrobial activity of MP-NSs, Fig. 10 offers a graphical depiction. This dataset provides valuable insights into the extent of inhibition exerted by the tested substances on the growth and activity of the selected microorganisms.

Taken together, the results from FT-IR, thermal analysis, SEM, and XRD studies strongly support the successful preparation of MP-NSs, wherein the drug is effectively entrapped in the nanosponge matrix, converting it from a crystalline state to an amorphous state. This formulation demonstrates promising potential for pharmaceutical applications due to its stability and drug entrapment capabilities.

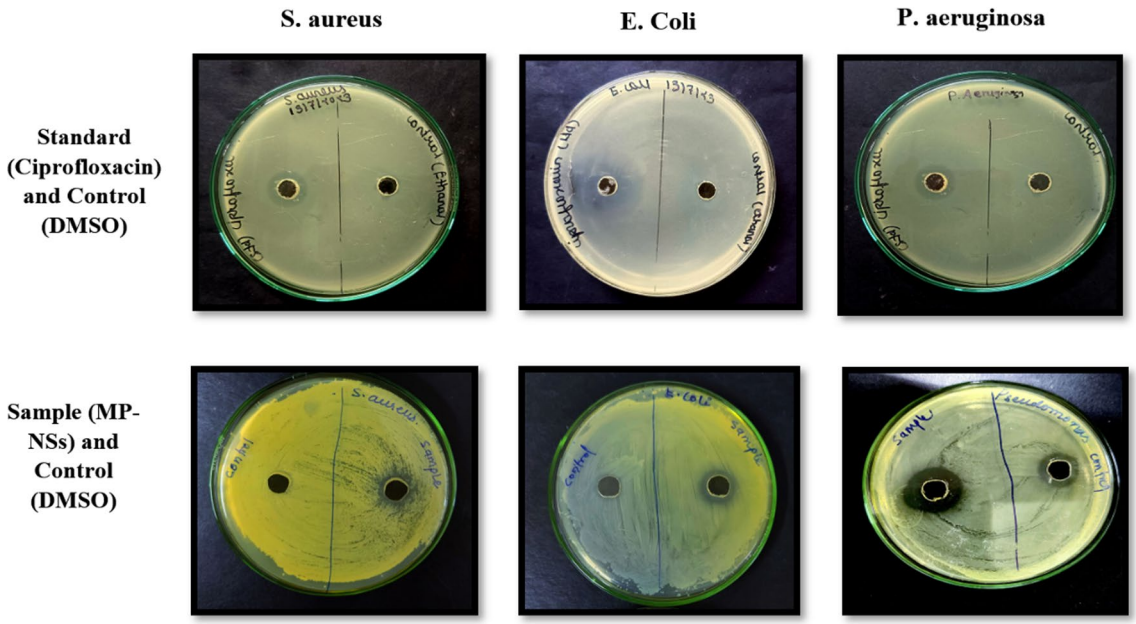

Fig. 9 ZOI of sample, control and standard against *SA, EC,* and *PA* (whereas ZOI—zone of inhibition, *SA- staphylococcus aureus, EC- Escherichia coli, PA- Pseudomonas aeruginosa*)

Table 5 Antimicrobial activity of Mupirocin-loaded nanosponges and zone of inhibition for Standard (Ciprofloxacin), Control (Dimethyl sulfoxide) and Sample Mupirocin solution

Organisms	Zone of inhibition (mm)		
	Standard (Ciprofloxacin)	Control (DMSO)	MP–nanosponges (10 mg/mL)
S. aureus	18	11	19
E. coli	20	8	17
P. aeruginosa	21	9	18

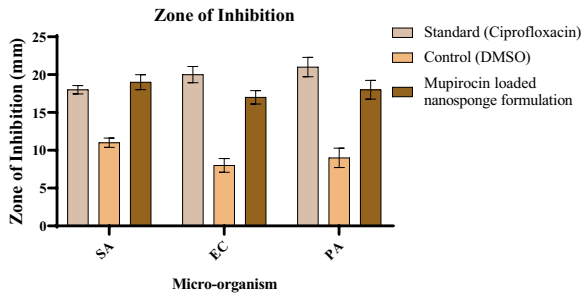

Fig. 10 Graphical representation of antimicrobial activity of mupirocin. Whereas, SA-*Staphylococcus aureus*, EC-*Escherichia coli*, and PA-*Pseudomonas aeruginosa*

Table 6 Evaluation parameters of MP-NSs gel

Parameters	MP-NSs gel formulation
Physical appearance	White and Opaque
pH	6.4 ± 0.03
Viscosity (cPs)	1026
Drug content (%w/w)	88.48 ± 0.04

Characterisation of nanosponges (MP-NSs) loaded gel

The developed carbopol gel formulations exhibited a uniform and smooth white texture, showcasing thixotropic properties that facilitated easy and efficient spreading. The pH value of the gel was quantified as 6.4 ± 0.03, and its viscosity was determined to be 1026 centipoises (cPs). Notably, the spreadability assessment of the gel containing MP-NSs yielded a value of 31.0 g·cm/sec, affirming its effective spreading capability. The drug content analysis revealed a value of 88.48 ± 0.04, indicating a uniform distribution of the drug within the gel matrix. These comprehensive findings are detailed in Table 6.

Skin irritation studies

The irritation assessment of the control with (0.9%w/v) NaCl, the control containing (1% w/v)

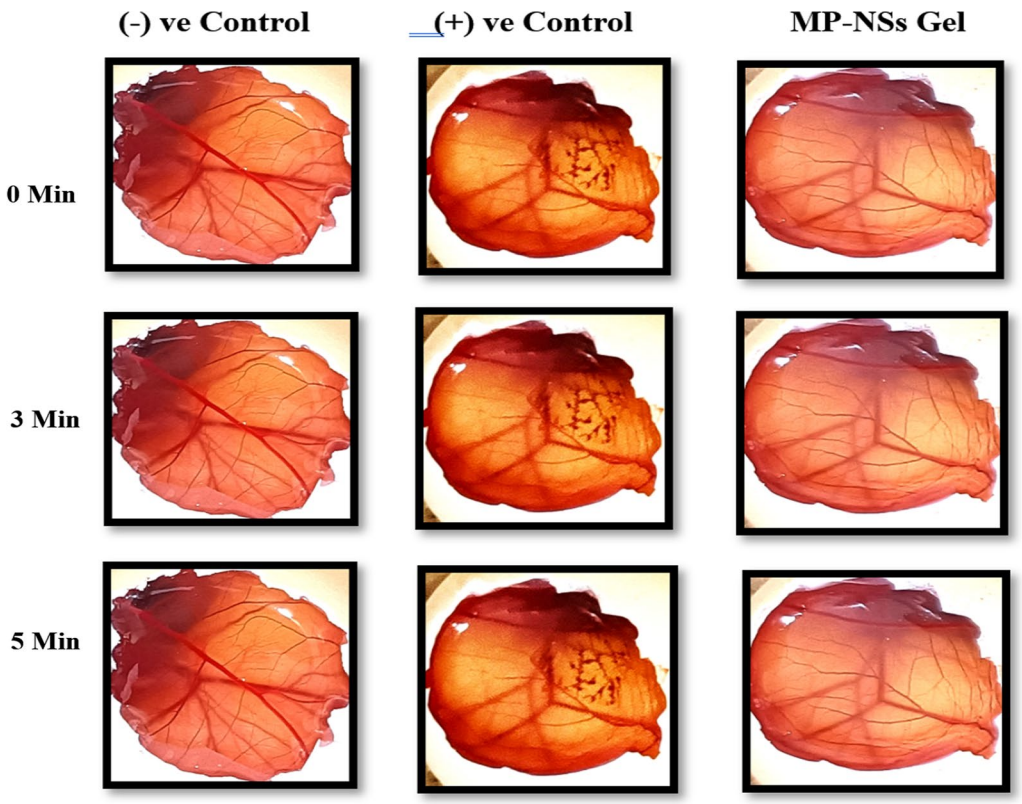

Fig. 11 Images showing the vascular effects of different substances applied on the chorioallantoic membrane over a period of 5 min. (1) Sodium chloride (0.9%w/v) (2) 0.1 N sodium hydroxide (3) MP-Nanosponge gel

Table 7 HET-CAM irritation score of the MP-NS Gel, NaOH (1%, positive control), and NaCl (0.9%, Negative control)

Samples		Score												
		Non-irritant		Mild irritant			Moderate Irritant			Severe Irritant		Overall Score
	Egg	Time (min)		Time (min)			Time (min)			Time (min)		
		0	0.5	2	5	0.5	2	5	0.5	2	5	0	0.5	2	5	
MP-NS Gel	Egg 1	0	0	0	0.0	0	0	0	0	0	0	0	0	0	0	
	Egg 2	0	0	0	0.0	0	0	0	0	0	0	0	0	0	0	
	Egg 3	0	0	0	0.2	0	0	0	0	0	0	0	0	0	0	
	Mean score	0	0	0	0.2	0	0	0	0	0	0	0	0	0	0	0
Positive Control (NaOH 1%)	Egg 1	0	0	0	0	0	0	0	0	0	0	0	14	17	19	
	Egg 2	0	0	0	0	0	0	0	0	0	0	0	16	18	19	
	Egg 3	0	0	0	0	0	0	0	0	0	0	0	16	18	20	
	Mean score	0	0	0	0	0	0	0	0	0	0	0	14.5	16.1	18.7	16.43
Negative Control (NS 0.9%)	Egg 1	0	0	0	0	0	0	0	0	0	0	0	0	0	0	
	Egg 2	0	0	0	0	0	0	0	0	0	0	0	0	0	0	
	Egg 3	0	0	0	0	0	0	0	0	0	0	0	0	0	0	
	Mean score	0	0	0	0	0	0	0	0	0	0	0	0	0	0	0

NaOH, and the formulated MP-NSs gel was conducted through the utilisation of the HET-CAM test. Figure 11 illustrates the effects on blood vessels caused by different substances applied to the chorioallantoic membrane within a 5-min interval. The evaluation of the scores from all the treated groups was performed at various time intervals, and the average irritation scores are presented in Table 7. The negative control sample exhibited a score of zero at each time interval (signifying absence of irritation, ranging from 0 to 0.8), while the positive control demonstrated an exceedingly high score (16.43). Similarly, the formulated MP-NSs gel also resulted in a score of zero, indicating an absence of irritation on the chorioallantoic membrane. The absence of irritation scores in the negative control and the formulated solution suggests that they do not cause irritation to the membrane, thus establishing their non-irritating nature to the skin.

In vitro drug release assay

The impact of composition and carrier on the drug release pattern of distinct formulations were examined using a cellulose dialysis membrane. The in vitro discharge patterns of MP from diverse formulations, as depicted in Fig. 12, demonstrated that MP ointment and MP cream released the MP within 4 and 10 h, respectively. In contrast, the MP-NSs gel exhibited a prolonged release extending up to a 24-h period. The release of the MP from the gel formulation was governed by a diffusion-controlled mechanism. The percentage of drug release is outlined in Table 8.

Table 8 Percent (%) drug released of marketed mupirocin ointment, mupirocin cream and prepared mupirocin-loaded nanosponge gel formulation

Time (hour)	Formulations (% Cumulative drug released)		
	Mupirocin ointment	Mupirocin cream	Mupirocin-loaded Nanosponge–Gel
0.5	39.81 ± 1.33	21.40 ± 1.31	8.17 ± 2.21
1	76.48 ± 2.41	39.50 ± 2.19	11.35 ± 1.21
2	84.47 ± 1.71	46.97 ± 2.85	15.30 ± 3.21
3	91.05 ± 3.57	55.95 ± 3.34	20.35 ± 2.21
4	95.51 ± 2.74	68.49 ± 1.79	27.69 ± 1.21
6	–	74.38 ± 2.11	42.15 ± 3.21
8	–	83.28 ± 1.42	47.15 ± 1.21
12	–	90.20 ± 3.64	58.60 ± 2.21
24	–	–	81.06 ± 2

[a] Each observation is the mean ± SD of three determinations

Ex vivo drug deposition assay

The quantity of mupirocin accumulated in excised rat abdominal skin through various formulations at distinct time intervals is illustrated in Fig. 13. The quantity of mupirocin deposited within the skin was notably greater when using the MP-NSs gel (211.4 ± 6.9 μg/cm^2) in comparison to the MP cream (83.57 ± 6.7 μg/cm^2) or MP ointment (34.03 ± 5.6 μg/cm2) after 24 h. This observation underscores that the nanosponges facilitated an enhancement in the drug residence in the skin.

Stability study

The results of the stability study, as shown in Table 9, revealed that the MP-NSs gel was found to be stable after a period of three months. Significant changes have not been seen when these were demonstrated for physical appearance, pH, and drug content at different temperature conditions (4 ± 2 °C, 25 ± 2 °C and 37 ± 2 °C). A drug

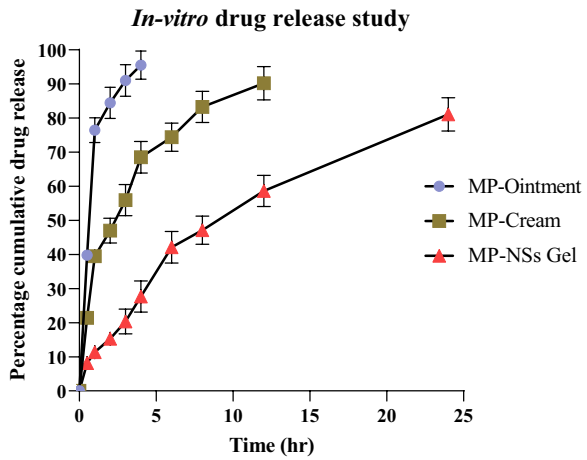

Fig. 12 In-vitro drug release of marketed formulation and prepared mupirocin-loaded nanosponge-gel formulation

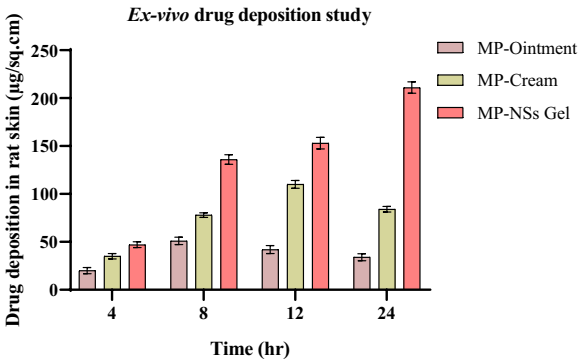

Fig. 13 Graphical representation of concentration of drug deposited in rat skin at different time intervals

Table 9 Results of stability studies of MP-NSs gel

Parameters	MP-NSs gel			
	Initial	After 3 months at 4 °C temperature	After 3 months at 25 °C temperature	After 3 months at 37 °C temperature
Physical appearance	White and opaque	No change	No change	No change
pH	6.3 ± 0.06	6.4 ± 0.03	6.2 ± 0.05	6.3 ± 0.04
Viscosity (Pa.s.)	1125 ± 6.93	1030 ± 3.46	1029 ± 5.29	1015 ± 6.57
Drug content (%)	88.48 ± 0.04	88.92 ± 0.34	87.54 ± 0.18	86.22 ± 0.03

content greater than 90% indicated acceptable NSs stability in gel.

In vivo wound healing study of MP-NSs gel and marketed formulation

DM was induced in rats through the I.P. delivery of STZ at a dosage of 60 mg/kg body weight. Blood samples were obtained using the retro-orbital method both prior to and subsequent to the STZ injection. These samples were subsequently analysed for blood glucose levels, C-reactive protein (CRP) levels, and glycated haemoglobin (HbA1C) levels, as documented in Table 10. The outcomes of these assessments provided confirmation of the successful induction of diabetes. Meanwhile, an excision wound model was employed to create wounds on the rat feet. These wounds were then exposed to various distinct treatments for further investigation and analysis. Table 11 presents the results of the wound closure percentages for different treatment groups. The diabetic wounds treated with standard Becaplermin gel exhibited the highest percentage of wound closure (96%), outperforming all the other groups. The diabetic wounds treated with MP-NSs gel showed a commendable wound closure rate of 92%, which was higher than the diabetic wound control group (43%), the normal wound control group (73.5%), DM group 4 treated with MP ointment (79%), and DM group 5 treated with MP cream (78%). The bar graph in Fig. 14 illustrates the percentage of wound closure on days 4, 8, 12, and 16 for all the groups. On day 4, there was a consistent and exponential wound healing rate observed across all groups. However, from day 8 onwards, both DM group 3 (diabetic wound treated with MP-NSs gel) and DM group 6 (diabetic wound treated with Becaplermin gel following MP-NSs gel) exhibited enhanced wound healing compared to the rest of the groups. Figure 15 clearly demonstrated that the diabetic wounds treated with Becaplermin gel exhibited a faster rate of healing compared to all the other groups. The diabetic control group, which did not receive any treatment, showed the slowest healing rate, even when compared to the normal wound control group. Surprisingly, the group with diabetic wounds treated with MP-NSs gel showed earlier and more improved wound healing compared to both the diabetic control group and the normal wound control group. Additionally, when compared to standard MP ointment and MP cream, the MP-NSs gel displayed faster wound closure. This difference in efficacy can be attributed to the sustained release property of the nanosponge-based gel. While the marketed conventional products required thrice-daily application, the MP-NSs gel was administered only once a day due to its sustained release characteristics, leading to superior results in wound healing. Overall, these findings strongly suggest that the MP-NSs gel had a significantly positive effect on accelerating wound healing in diabetic rats. Its sustained release properties not only contributed to better efficacy compared to the conventional products but also facilitated once-daily delivery, simplifying the treatment protocol. These findings demonstrate that the MP-NSs gel was highly effective in promoting wound closure in diabetic rats, with a significant improvement over the untreated diabetic wounds and the control groups treated with MP ointment and MP cream. The standard Becaplermin gel displayed the highest wound closure percentage, but the MP-NSs gel showed a promising and competitive efficacy, making it a potential alternative treatment option for diabetic wound healing.

Discussion

The study aimed to develop Mupirocin-loaded nanosponges using the emulsion solvent diffusion method, an alternative and promising approach for nanosponge preparation. This method offers advantages such as simplicity, reproducibility, and rapidity, while also

Table 10 Confirmation of induction of diabetes mellitus in rats

Blood test	Results	
	Before STZ IP injection	After 72 h
Random blood glucose level (mg/dL)	67	369
HbA1C level (%)	6.6	9.6
CRP level (mg/L)	1.3	6.2

Table 11 Tabular representation of percentage wound closure whereas

Days	% Wound closure					
	NWC	DWC	DW + MP-NSs Gel	DW + MP Ointment	DW + MP-Cream	DW + Becaplermin gel
4	16.2	5.9	24.2	23.3	23.5	25.3
8	31.3	19.4	39.1	35.1	35.8	42.7
12	49.1	24.8	52.7	48.7	49.2	53.4
14	63.7	37.4	71.8	62.5	61.2	78.9
16	73.5	43.1	92.5	79.8	78.7	96.1

NWC Normal wound control, *DWC* Diabetic wound control, *DW Group 1* Diabetic wound treated with mupirocin-loaded nanosponge gel, *DW Group 2* Diabetic wound treated with MP-ointment, *DW Group 3* Diabetic wound treated with MP-cream, *DW Group 4* Diabetic wound treated with Becaplermin gel

avoiding the use of toxic solvents. To optimise the nanosponge formulation, a factorial design with EC concentration and stirring rate as independent variables was employed. The results demonstrated the significant influence of these variables on PY, EE, and MPS of the nanosponges.

Regarding MP entrapment efficiency (%EE), increasing the EC concentration positively impacted %EE, meaning that higher EC concentrations led to improved drug entrapment within the nanosponges. Conversely, higher stirring rates had a negative effect on %EE, indicating that excessive stirring negatively influenced drug entrapment. For production yield, both EC concentration and stirring rate had a positive influence, contributing to higher yields of nanosponges. The MPS of the nanosponges was influenced positively by EC concentration but negatively by stirring rate. This indicates that higher EC concentrations and lower stirring rates resulted in larger nanosponge particle sizes.

The FT-IR analysis provided insights into the interactions between mupirocin, ethyl cellulose, and carbopol, confirming the stability of the formulations. The thermal analysis and X-ray diffraction (XRD) data confirmed the successful entrapment of mupirocin within the nanosponges, converting it from a crystalline to an amorphous state. The nanosponge formulation (F9) showed promising properties, including an MPS of 189 nm and a zeta potential of (−) 26 mV, indicating a stable and effective nanosponge formulation. The nanosponge-gel exhibited sustained drug release for up to 24 h, providing potential advantages in controlled drug delivery. The nanosponge formulation demonstrated improved drug deposition in excised rat abdominal skin compared to conventional formulations like ointment and cream. The HET-CAM irritation study indicated that the nanosponge-gel was non-irritant, making it a safe formulation for topical application. The stability study revealed that the nanosponge-gel remained stable over a three-month period, with a drug entrapment efficiency greater than 90%, suggesting the potential for long-term shelf life.

The in vivo study on diabetic rat wounds demonstrated that the nanosponge-gel significantly accelerated wound healing compared to conventional products and even outperformed MP ointment and MP cream. The sustained release property of the nanosponge-gel facilitated once-daily delivery and provided improved wound closure efficacy. while the gel fostered an optimally humid environment conducive to wound care during the final stages of wound healing and sealing [46].

The acceleration of wound healing is primarily attributed to Mupirocin, which plays a pivotal role in stimulating the production of growth factors and the proliferation of human keratinocytes [18]. Additionally, the nanosponges, due to their smaller size, exhibit enhanced penetration capabilities into deeper tissues at the injured site. The gel component of the formulation fosters an optimally humid environment, particularly beneficial during the final stages of wound healing and sealing. Therefore, the combined efficacy of Mupirocin-loaded nanosponge

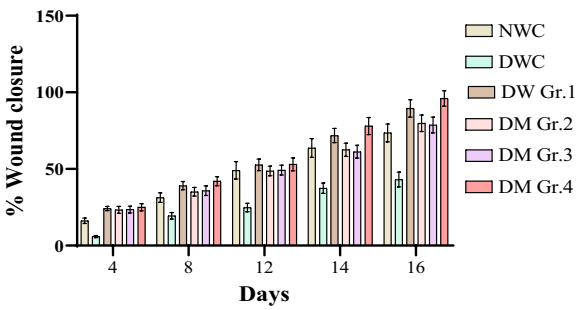

Fig. 14 Graphical representation of percentage wound closure whereas, NWC- normal wound control, DWC- diabetic wound control, DW Group 1 -diabetic wound treated with mupirocin-loaded nanosponge gel, DW Group 2- Diabetic wound treated with MP-Ointment, DW Group 3- Diabetic wound treated with MP-Cream, DW Group 4- Diabetic wound treated with Becaplermin gel

Fig. 15 Photographic representation of wound healing and closure of different animal groups

gel as a dosage form significantly contributes to the overall acceleration of the wound healing process.

Overall, the results of this study indicate successful development of mupirocin-loaded nanosponges using the emulsion solvent diffusion method, providing a potential alternative for wound healing in diabetic rats. The nanosponge-gel exhibited favourable properties, including sustained drug release, enhanced drug deposition within the skin, stability, and non-irritating characteristics. This novel formulation has promising potential for pharmaceutical applications and merits further investigation for potential clinical translation as an effective and convenient treatment option for wound healing.

Conclusion

A novel drug delivery system utilising mupirocin-loaded nanosponges has been successfully developed to facilitate once-a-day sustained release medication for the topical treatment of diabetic wounds. The innovative formulations demonstrated improved drug retention within the skin, showcasing the superior potential of the nanosponge-based delivery system when compared to conventional mupirocin ointments and creams available in the market. Considering the heightened effectiveness and the enhanced patient adherence due to reduced application frequency, it is evident that the nanosponge-based gel formulations will play a substantially more beneficial role in the treatment of diabetic wounds.

Abbreviations

DM	Diabetes mellitus
T2DM	Type 2 diabetes mellitus
DFU	Diabetic foot ulcer
DWC	Diabetic wound control
MP	Mupirocin
NSs	Nanosponges
EC	Ethyl cellulose
PVA	Polyvinyl alcohol
DCM	Dichloromethane
CP 934	Carbopol 934
STZ	Streptozotocin
I.P	Intraperitoneal
DMSO	Dimethyl sulfoxide
ESD	Emulsion solvent diffusion
MP-NSs	Mupirocin-loaded nanosponges
ANOVA	Analysis of variance
FT-IR	Fourier transform infrared
DSC	Differential scanning calorimetry
XRD	X-Ray diffraction
SEM	Scanning electron microscopy

%PY	Per cent production yield
%EE	Per cent entrapment efficiency
MPS	Mean particle size
NaCL	Sodium chloride
NaOH	Sodium hydroxide
HET-CAM	Hen's Egg Test-Chorioallantoic Membrane
ZOI	Zone of inhibition
RT	Room temperature
CFU	Colony forming units
NBH	Nutrition Broth Medium
mL	Millilitre
min	Minutes
hrs.	Hours
g	Gram
µm	Micrometer
rpm	Rotation per minute
°C/min	Degree Celsius per minute
Cm	Centimetre
cm^{-1}	Per centimetre
Conc.	Concentration

Acknowledgements
The content is solely the responsibility of the authors.

Author contributions
RSD and PSS have taken efforts to design the study. RSD did experimental, DRT, PAR, and DSW helped in execution of study. All the authors have taken efforts to develop and evaluate the formulation. RSD have interpreted the data obtained during the study. RSD and PSS drafted, and reviewed the manuscript for further communications.

Funding
Not applicable.

Availability of data and materials
All data and material are available upon request.

Declarations

Ethics approval and consent to participate
The manuscript is solely submitted to this journal and has not been sent elsewhere simultaneously. The content is original, never published before, and complies with ethical standards. Results are presented transparently, without manipulation. Data acquisition adheres to discipline-specific guidelines. The study's experimental procedure received approval from the Animal Ethics Committee of Department of Pharmaceutical Sciences, RTMNU, Nagpur (Approval number IAEC/UDPS/2022/02/08), following Indian Committee for the Purpose of Control and Supervision of Experiments with Animals (CPCSEA) specifications.

Consent for publication
Yes.

Competing interests
The authors declare that they have no competing interests.

Author details
[1]Department of Pharmaceutical Sciences, Rashtrasant Tukadoji Maharaj Nagpur University, Nagpur, Maharashtra 44003, India.

Received: 18 August 2023 Accepted: 21 February 2024
Published online: 04 March 2024

References

1. Deshpande A, Harris-Hayes M, Schootman M (2008) Epidemiology of diabetes and diabetes-related complications. Phys Ther 88(11):1254–1264
2. Kharroubi AT, Darwish HM (2015) Diabetes mellitus: the epidemic of the century. World J Diabetes 6(6):850
3. Galicia-Garcia U, Benito-Vicente A, Jebari S, Larrea-Sebal A, Siddiqi H, Uribe KB, Ostolaza H, Martín C (2020) Pathophysiology of type 2 diabetes mellitus. Int J Mol Sci 21(17):6275
4. Kumar A, Gangwar R, Zargar A, Kumar R, Sharma A (2023) Prevalence of diabetes in India: a review of IDF diabetes atlas 10th edition. Curr Diabetes Rev 20(1):e130423215752
5. Ong KL, Stafford LK, McLaughlin SA, Boyko EJ, Vollset SE, Smith AE, Dalton BE, Duprey J, Cruz JA, Hagins H, Lindstedt PA (2023) Global, regional, and national burden of diabetes from 1990 to 2021, with projections of prevalence to 2050: a systematic analysis for the global burden of disease study 2021. The Lancet 402(10397): 203–234
6. Alexiadou K, Doupis J (2012) Management of diabetic foot ulcers. Diabetes Ther 3:1–5
7. Jodheea-Jutton A, Hindocha S, Bhaw-Luximon A (2022) Health economics of diabetic foot ulcer and recent trends to accelerate treatment. Foot 1(52):101909
8. Syafril S (2018) Pathophysiology diabetic foot ulcer. In: IOP Conference series: earth and environmental science (Vol. 125, No. 1, p. 012161). IOP Publishing
9. Del Core MA, Ahn J, Lewis RB III, Raspovic KM, Lalli TA, Wukich DK (2018) The evaluation and treatment of diabetic foot ulcers and diabetic foot infections. Foot Ankle Orthop 3(3):2473011418788864
10. Zhang P, Lu J, Jing Y, Tang S, Zhu D, Bi Y (2017) Global epidemiology of diabetic foot ulceration: a systematic review and meta-analysis. Ann Med 49(2):106–116
11. Wang X, Yuan CX, Xu B, Yu Z (2022) Diabetic foot ulcers: classification, risk factors and management. World J Diabetes 13(12):1049
12. Afonso AC, Oliveira D, Saavedra MJ, Borges A, Simões M (2021) Biofilms in diabetic foot ulcers: Impact, risk factors and control strategies. Int J Mol Sci 22(15):8278
13. Jalilian M, Ahmadi Sarbarzeh P, Oubari S (2020) Factors related to severity of diabetic foot ulcer: a systematic review. Diabetes Metab Syndr Obes 25:1835–1842
14. Rai V, Moellmer R, Agrawal DK (2022) Clinically relevant experimental rodent models of diabetic foot ulcer. Mol Cell Biochem 477(4):1239–1247
15. Ezhilarasu H, Vishalli D, Dheen ST, Bay BH, Srinivasan DK (2020) Nanoparticle-based therapeutic approach for diabetic wound healing. Nanomaterials 10(6):1234
16. Sutherland R, Boon RJ, Griffin KE, Masters PJ, Slocombe B, White AR (1985) Antibacterial activity of mupirocin (pseudomonic acid), a new antibiotic for topical use. Antimicrob Agents Chemother 27(4):495–498
17. Pappa KA (1990) The clinical development of mupirocin. J Am Acad Dermatol 22(5):873–879
18. Twilley D, Reva O, Meyer D, Lall N (2022) Mupirocin promotes wound healing by stimulating growth factor production and proliferation of human keratinocytes. Front Pharmacol 11(13):862112
19. Gangwar A, Kumar P, Singh R, Kush P (2021) Recent advances in mupirocin delivery strategies for the treatment of bacterial skin and soft tissue infection. Future Pharmacol 1(1):80–103
20. Girigoswami A, Girigoswami K (2022) Versatile applications of nanosponges in biomedical field: a glimpse on SARS-CoV-2 management. BioNanoScience 12(3):1018–1031
21. Jagtap SR, Bhusnure OG, Mujewar IN, Gholve SB, Panchabai VB (2019) Nanosponges: a novel trend for targeted drug delivery. J Drug Deliv Ther 9(3s):931–938
22. Moin A, Roohi NF, Rizvi SM, Ashraf SA, Siddiqui AJ, Patel M, Ahmed SM, Gowda DV, Adnan M (2020) Design and formulation of polymeric nanosponge tablets with enhanced solubility for combination therapy. RSC Adv 10(57):34869–34884
23. Sharma R, Pathak K (2011) Polymeric nanosponges as an alternative carrier for improved retention of econazole nitrate onto the skin through topical hydrogel formulation. Pharm Dev Technol 16(4):367–376
24. Pandit AP, Patel SA, Bhanushali VP, Kulkarni VS, Kakad VD (2017) Nebivolol-loaded microsponge gel for healing of diabetic wound. AAPS PharmSciTech 18(3):846–854
25. Ahmed MM, Fatima F, Anwer MK, Ibnouf EO, Kalam MA, Alshamsan A, Aldawsari MF, Alalaiwe A, Ansari MJ (2021) Formulation and in vitro

evaluation of topical nanosponge-based gel containing butenafine for the treatment of fungal skin infection. Saudi Pharm J 29(5):467–477
26. Iriventi P, Gupta NV, Osmani RA, Balamuralidhara V (2020) Design & development of nanosponge loaded topical gel of curcumin and caffeine mixture for augmented treatment of psoriasis. DARU J Pharm Sci 28:489–506
27. Kumar PM, Ghosh A (2015) Development and evaluation of metronidazole loaded microsponge based gel for superficial surgical wound infections. J Drug Deliv Sci Tech 30:15–29
28. Srivastava S, Mahor A, Singh G, Bansal K, Singh PP, Gupta R, Dutt R, Alanazi AM, Khan AA, Kesharwani P (2021) Formulation development, in vitro and in vivo evaluation of topical hydrogel formulation of econazole nitrate-loaded β-cyclodextrin nanosponges. J Pharm Sci 110(11):3702–3714
29. Sareen R, Nath K, Jain N, Dhar KL (2014) Curcumin loaded microsponges for colon targeting in inflammatory bowel disease: fabrication, optimization, and in vitro and pharmacodynamic evaluation. Biomed Res Int 1:2014
30. Srivastava R, Kumar D, Pathak K (2012) Colonic luminal surface retention of meloxicam microsponges delivered by erosion-based colon-targeted matrix tablet. Int J Pharm 427(2):153–162
31. Banu A, Hassan MM, Rajkumar J, Srinivasa S (2015) Spectrum of bacteria associated with diabetic foot ulcer and biofilm formation: a prospective study. Australas Med J 8(9):280
32. Barry BW, Meyer MC (1979) The rheological properties of carbopol gels I. Continuous shear and creep properties of carbopol gels. Int J Pharm 2(1):1–25
33. Yadav V, Jadhav P, Dombe S, Bodhe A, Salunkhe P (2017) Formulation and evaluation of microsponge gel for topical delivery of antifungal drug. Int J Appl Pharm 13:30–37
34. Amrutiya N, Bajaj A, Madan M (2009) Development of microsponges for topical delivery of mupirocin. AAPS PharmSciTech 10:402–409
35. Echevarría L, Blanco-Prieto MJ, Campanero MA, Santoyo S, Ygartua P (2003) Development and validation of a liquid chromatographic method for in vitro mupirocin quantification in both skin layers and percutaneous penetration studies. J Chromatogr B 796(2): 233-41
36. Zafar A, Imam SS, Alruwaili NK, Yasir M, Alsaidan OA, Alshehri S, Ghoneim MM, Khalid M, Alquraini A, Alharthi SS (2022) Formulation and evaluation of topical nano-lipid-based delivery of butenafine: in vitro characterization and antifungal activity. Gels 8(2):133
37. Interagency coordinating committee on the validation of alternative methods (ICCVAM) (2010) ICCVAM-recommended test method protocol: hen's egg test—chorioallantoic membrane (HET-CAM) test method. ICCVAM Test Method Eval Rep 13: B30–8
38. Kumar S, Prasad M, Rao R (2021) Topical delivery of clobetasol propionate loaded nanosponge hydrogel for effective treatment of psoriasis: formulation, physicochemical characterization, antipsoriatic potential and biochemical estimation. Mater Sci Eng C 1(119):111605
39. Szkudelski T (2012) Streptozotocin–nicotinamide-induced diabetes in the rat. Characteristics of the experimental model. Exp Biol Med 237(5):481–490
40. Cruz PL, Moraes-Silva IC, Ribeiro AA, Machi JF, de Melo MD, Dos Santos F, da Silva MB, Strunz CM, Caldini EG, Irigoyen MC (2021) Nicotinamide attenuates streptozotocin-induced diabetes complications and increases survival rate in rats: role of autonomic nervous system. BMC Endocr Disord 21(1):1
41. Mythili MD, Vyas R, Akila G, Gunasekaran S (2004) Effect of streptozotocin on the ultrastructure of rat pancreatic islets. Microsc Res Tech 63(5):274–281
42. Akbarzadeh A, Norouzian D, Mehrabi MR, Jamshidi SH, Farhangi A, Verdi AA, Mofidian SM, Rad BL (2007) Induction of diabetes by streptozotocin in rats. Indian J Clin Biochem 22:60–64
43. Ghasemi A, Jeddi S (2023) Streptozotocin as a tool for induction of rat models of diabetes: a practical guide. EXCLI J 22:274
44. Kandhare AD, Ghosh P, Bodhankar SL (2014) Naringin, a flavanone glycoside, promotes angiogenesis and inhibits endothelial apoptosis through modulation of inflammatory and growth factor expression in diabetic foot ulcer in rats. Chem Biol Interact 5(219):101–112
45. Masson-Meyers DS, Andrade TA, Caetano GF, Guimaraes FR, Leite MN, Leite SN, Frade MA (2020) Experimental models and methods for cutaneous wound healing assessment. Int J Exp Pathol 101(1–2):21–37
46. Landsman A, Agnew P, Parish L, Joseph R, Galiano RD (2010) Diabetic foot ulcers treated with becaplermin and TheraGauze, a moisture-controlling smart dressing: a randomized, multicenter, prospective analysis. J Am Podiatr Med Assoc 100(3):155–160

Publisher's Note